GPH-International Journal of Mechanical And Civil Engineering
(E-ISSN: 3050-967X)
Volume 08 | Issue 01 | January-June 2026
Published by: Global Publication House
DOI: https://doi.org/10.5281/zenodo.23856320
Available online at www.gphjournal.org
Journal homepage: https://gphjournal.org/index.php/mce/index

Design, Fabrication, and Performance Evaluation of a Locally Developed Automotive Engine Test Bed Using a Hydraulic Water-Brake Dynamometer

Gregory, A. Dolor[1] & Esabunor Temabor[2]
[1]Mechanical Department, School of Engineering, Delta State Polytechnic, P.M.B. 03, Otefe- Oghara, Delta State, Nigeria.
[2]Welding and Fabrication Department, School of Engineering, Delta State Polytechnic, P.M.B. 03, Otefe- Oghara, Delta State, Nigeria.
E-mail address: dolorgregory@gmail.com

Abstract

The high cost of commercial automotive engine test facilities limits access to reliable engine performance testing equipment in many Nigerian tertiary institutions, thereby constraining practical engineering training and experimental research. This study aimed to design, construct and evaluate a locally fabricated automotive engine test bed incorporating a hydraulic water-brake dynamometer. The test bed was designed for four-cylinder petrol engines with displacement capacities of 1.2-2.0 L, a design power absorption rating of 90 kW and a maximum design torque of 220 N·m. The supporting frame was fabricated from mild steel, while torque was measured using a strain-gauge load cell mounted on a 500 mm moment arm. Engine speed was measured using an optical tachometer, and temperature and fuel-consumption measurements were incorporated into the instrumentation system. The test bed was evaluated using a Toyota 7A-FE, 1.8 L, four-cylinder petrol engine under full-load conditions between 1,000 and 5,500 rpm and at different throttle openings at 3,000 rpm. The results showed a maximum recorded torque of 135.5 N·m at 3,000 rpm and a maximum calculated brake power of approximately 56.0 kW at 5,000 rpm. During part-load testing, torque and brake power increased with increasing throttle opening. The reported direct material cost was ₦286,500, excluding labour and overheads. The findings demonstrate the feasibility of locally fabricating an engine test bed for steady-state performance evaluation and engineering education. Further validation is required to verify fuel-consumption and efficiency calculations and to establish the test bed's full design capacity experimentally.

Keywords

Automotive engine; engine test bed; hydraulic water-brake dynamometer; brake power; torque measurement; local fabrication.

© 2026 Author(s). Published by Global Publication House (GPH).
This is an Open Access article distributed under the terms of the CC BY 4.0 License.

1. Introduction

Internal combustion engines remain important power sources in road transportation and continue to require reliable performance testing for engine development, maintenance, fault diagnosis and engineering education. Although modern automotive technologies are increasingly incorporating electrification, petrol-powered engines remain relevant in many vehicle fleets, particularly in developing economies where used vehicles constitute a substantial proportion of vehicles in service. The ability to determine engine torque, brake power and fuel consumption under controlled operating conditions is essential for evaluating engine performance and identifying deviations from expected operating characteristics. Engine dynamometer testing provides a systematic means of obtaining these parameters and examining their variation with engine speed and load. The International Organization for Standardization (ISO) specifies procedures for determining engine net power and presenting performance characteristics, including power and specific fuel consumption as functions of engine speed under full-load conditions (ISO, 2020).

An engine test bed integrates the engine under investigation with a dynamometer, supporting structure, power transmission system, and fuel supply and measurement instrumentation. The dynamometer applies a controllable load to the engine, while torque and rotational speed measurements provide the basis for calculating brake power. Additional measurements of fuel consumption enable the determination of brake-specific fuel consumption (BSFC) and brake thermal efficiency. These parameters provide complementary information about the ability of an engine to convert the chemical energy of fuel into useful mechanical output. Their accurate determination depends on appropriate instrumentation, calibration, stable operating conditions and a consistent test procedure. ISO 15550:2016 provides general requirements for engine power determination, including reference conditions and methods for declaring power and fuel consumption, while ISO 1585:2020 addresses net-power testing of road-vehicle engines (ISO, 2016, 2020). Consequently, the design of a functional engine test bed must consider not only the mechanical capacity of the dynamometer but also measurement accuracy, thermal management, shaft alignment, structural integrity and operational safety.

Several dynamometer technologies are available for engine testing, including friction-brake, hydraulic, eddy-current and regenerative dynamometers. The selection of a suitable system depends on the engine's power and torque requirements, the desired degree of load control, measurement precision, maintenance requirements and available financial resources. Hydraulic, or water-brake, dynamometers absorb mechanical energy through fluid motion and shear within a rotor-housing assembly, with the absorbed energy dissipated principally as heat in the working fluid. Their relatively straightforward operating principle and suitability for sustained steady-state loading make them attractive for engine laboratories and experimental facilities. However, adequate water circulation, reliable torque measurement, appropriate rotor and shaft design, and effective guarding of rotating components remain essential for satisfactory operation. Previous work on water-brake dynamometer development has demonstrated the feasibility of constructing and experimentally evaluating such systems for engine performance testing (Romandoni et al., 2021).

Access to functional laboratory equipment is also an important consideration in engineering education and applied research. In resource-constrained institutions, the cost of acquiring imported

experimental apparatus may limit students' opportunities to undertake practical measurements and may restrict researchers' ability to conduct experimental investigations. Local design and manufacture offer a potential alternative by combining engineering analysis, locally accessible materials and existing workshop capabilities. Ojobor and Chidi (2008), in their work on the design, manufacture and characterisation of a journal-bearing demonstration unit, demonstrated the potential for indigenous laboratory-equipment development within Nigerian engineering institutions. More recently, Alabi et al. (2025) reported the development of a force-table apparatus using locally available materials, illustrating the continuing relevance of cost-conscious experimental-equipment design in engineering education. These studies support the broader case for developing laboratory apparatus that can be fabricated, maintained and adapted to local institutional requirements. Nevertheless, a locally manufactured engine test bed must be assessed through actual operation and calibrated measurements rather than judged solely by its design calculations or fabrication cost.

The present study focuses on the design, construction and performance evaluation of an automotive engine test bed for the Department of Mechanical Engineering Technology at Delta State Polytechnic, Otefe, Oghara, Nigeria. The study addresses the need for an accessible experimental facility capable of supporting engine-performance measurements and practical training. The developed system incorporates a welded mild-steel support frame, a hydraulic water-brake dynamometer, a propeller-shaft transmission arrangement and instrumentation for measuring engine speed, reaction force and fuel consumption. A Toyota 7A-FE, 1.8-litre, four-cylinder petrol engine was selected for experimental evaluation. The investigation involved full-load tests over a range of engine speeds and part-load tests at a fixed engine speed, with the objective of examining the relationship between operating conditions and measured performance parameters.

The principal contribution of the study is the integration of locally fabricated mechanical components and calibrated measurement instrumentation into an automotive engine test bed, followed by experimental evaluation using an in-service petrol engine. In addition to documenting the design and construction process, the study examines the measured torque and brake-power characteristics, fuel-consumption behaviour and the potential application of the facility in engineering laboratory instruction and further engine-performance investigations. The work therefore provides a practical case study of locally developed engine-testing equipment and establishes a basis for subsequent improvements in instrumentation, data acquisition and experimental validation. Its findings are intended to inform the development of affordable engine-testing facilities in institutions where access to commercial dynamometer systems may be constrained by cost and maintenance considerations.

2. Materials and Methods

2.1 Research Design and Study Location

This study adopted an experimental engineering design involving the design, fabrication, and calibration and performance evaluation of an automotive engine test bed. The work was undertaken in the Department of Mechanical Engineering Technology workshop at Delta State Polytechnic, Otefe, Oghara, Nigeria. The experimental programme was designed to assess the functionality of the fabricated test bed and characterise the performance of a petrol engine under full-load and part-

load operating conditions. The methodology comprised mechanical design and component fabrication, system assembly, instrumentation calibration, engine performance testing and mathematical analysis of the experimental measurements.

The experimental approach followed established engine-dynamometer testing principles, in which engine speed, output torque and fuel consumption are measured under controlled operating conditions to determine brake power and fuel-efficiency parameters. The procedures were informed by ISO 1585:2020 and published work on the design and experimental assessment of water-brake dynamometers (ISO, 2020; Romandoni et al., 2021). However, the test procedure should be regarded as a laboratory performance evaluation rather than a claim of full compliance with the complete ISO certification procedure.

2.2 Materials and Equipment

The test bed was constructed using locally obtainable engineering materials and automotive components. The principal materials included mild steel rectangular hollow sections (RHS), mild steel plates, grey cast iron for the dynamometer housing, EN 8 carbon steel for the dynamometer shaft, rubber isolation mounts and a serviceable automotive propeller shaft. Standard mechanical fasteners, bearings, seals, water-control valves and electrical components were used for assembly and instrumentation. The main structural frame was fabricated from $100 \times 100 \times 8\ mm$ mild steel RHS, with a 10 mm thick mild steel base plate. Cross-bracing was provided using $75 \times 75 \times 6\ mm$ RHS. The hydraulic dynamometer incorporated a 280 mm diameter rotor with curved vanes, enclosed in grey cast iron housing. The power transmission system comprised a Toyota Land Cruiser propeller shaft fitted with universal joints. The engine was mounted on rubber isolation mounts to reduce the transmission of vibration to the supporting frame.

The principal measurement equipment comprised an optical tachometer (Lutron DT-2234C), a strain-gauge load cell with a digital display, a 500 mm torque-measurement arm, a graduated 5 L fuel burette, a stopwatch and Type K thermocouples with digital temperature indicators. An oil-pressure gauge was also installed for monitoring engine lubrication during operation. The dynamometer was supplied with cooling water from a 60 L header tank through manually operated valves. The nominal design parameters of the test bed were a maximum absorption capacity of 90 kW, a design torque capacity of 220 N·m and a maximum design speed of 6,500 rpm.

2.3 Material Selection

The materials used in the fabrication of the automotive engine test bed were selected based on their mechanical strength, rigidity, wear resistance, machinability, availability and cost. Table 1 presents the materials selected for this study while Table shows the Bill of Engineering Measurement and Evaluation. Mild-steel rectangular hollow sections ($100 \times 100 \times 8\,mm$) were selected for the main supporting frame because of their structural strength and suitability for fabrication by welding. A 10 mm-thick mild-steel plate was used for the base plate to provide a rigid mounting platform, while $75 \times 75 \times 6\ mm$ mild-steel sections were used for bracing to improve structural stability. Grey cast iron was selected for the dynamometer housing because of its rigidity, vibration-damping characteristics and suitability for housing the water-brake assembly. Mild-steel plate and flat bars were used to fabricate the rotor and vanes, respectively. An EN 8 carbon-steel shaft was

selected to transmit torque between the rotating components, while bearings mounted in plummer blocks supported shaft rotation. A serviceable automotive propeller shaft with universal joints was used to transmit power from the engine to the dynamometer. The selection of these materials and components was also guided by local availability, ease of machining and assembly, and the need to minimise fabrication costs while maintaining functional reliability.

Table 1 Selected material and their properties for major test bed components

Component	Material	Key Properties	Justification
Main frame members	100×100×8 mm mild steel RHS	Yield strength 275 MPa; weldable; good stiffness/weight	Standard stock; strong and stiff for frame duty
Frame base plate	Mild steel plate 10 mm	Yield strength 250 MPa; flat and weldable	Provides flat mounting datum for all components
Dynamometer rotor	Mild steel plate and flat bar	Adequate strength; weldable; balanced by machining	Weldable; available; machinable for balancing
Dynamometer housing	Grey cast iron GG20	Good castability; vibration damping; machinable	Cast to shape; good damping reduces vibration transmission
Moment arm	Mild steel flat bar 50×25 mm	Yield strength 250 MPa; stiff in bending	Simple to fabricate; adequate section stiffness
Shaft	Carbon steel (EN 8, 35 mm diameter)	Yield strength 460 MPa; good fatigue resistance	Higher strength required for rotating shaft in torsion

Guard	Mild steel sheet 1.5 mm	Adequate for enclosure; formable	Low cost; sufficient for safety guarding
Trunnion bearings	SKF 6207 deep groove ball bearings	Dynamic load 25.7 kN; speed rating 9,500 rpm	Standard bearing with adequate load/speed rating
Engine mounts	Rubber-in-shear sandwich mounts, 300 kg rating	Stiffness 200 N/mm; damping ratio 0.15	Isolates engine vibration from frame and instruments

Table 2 Bill of materials for the engine test bed (BEME)

S/N	Item	Qty	Unit	Unit Cost (₦)	Total (₦)
1	100×100×8 mm mild steel RHS	22	Metres	2,800	61,600
2	Mild steel plate 10 mm (base plate, pads)	2.0	m²	9,500	19,000
3	75×75×6 mm mild steel RHS (bracing)	8	Metres	2,000	16,000
4	Mild steel plate 20 mm (rotor disc blank)	1	Piece	8,500	8,500
5	Mild steel flat bar 80×20 mm (rotor vanes)	3	Metres	1,200	3,600
6	EN 8 carbon steel bar 40 mm dia (shaft)	0.5	Metres	6,500	3,250

7	Grey cast iron dynamometer housing (foundry)	1	Set	35,000	35,000
8	SKF 6207 bearings in SAF 207 plummer blocks	2	Sets	8,500	17,000
9	Toyota propeller shaft (used, serviceable)	1	Piece	12,000	12,000
10	Rubber isolation mounts, 300 kg, 200 N/mm	4	Pieces	3,500	14,000
11	500 N strain gauge load cell (HX711)	1	Piece	6,500	6,500
12	Digital panel meter for load cell	1	Piece	4,200	4,200
13	Optical tachometer (Lutron DT-2234C)	1	Piece	8,500	8,500
14	Type K thermocouples with digital indicators (2 off)	2	Sets	4,500	9,000
15	Oil pressure gauge 0-6 bar	1	Piece	2,500	2,500
16	Graduated Pyrex burette 5L	1	Piece	8,500	8,500
17	3-way fuel valve, fittings, copper tubing	1	Set	4,500	4,500
18	Header tank (60 L, GRP)	1	Piece	7,500	7,500
19	Globe valves 25 mm BSP (x3)	3	Pieces	2,200	6,600
20	Flexible exhaust bellows 63 mm	1	Piece	6,500	6,500
21	Mild steel sheet 1.5 mm (guard)	0.6	m^2	3,800	2,280

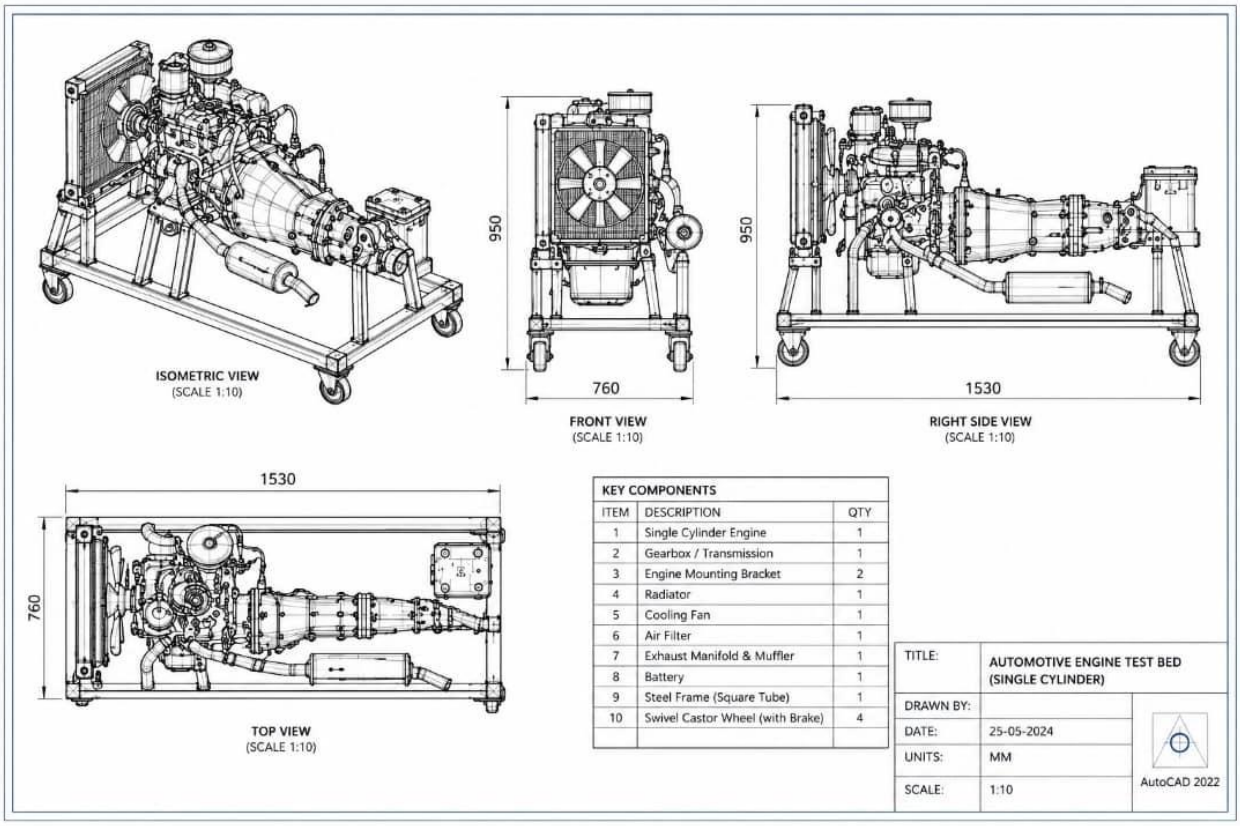
22	Instrumentation panel, switches, relays, wiring	1	Lot	18,500	18,500
23	MIG welding wire 1.0 mm (2 reels)	2	Reels	4,500	9,000
24	Bolts, nuts, washers (M10, M16, M20 assorted)	1	Lot	8,500	8,500
25	Paint (red oxide primer, enamel)	1	Lot	4,500	4,500
26	Levelling feet M20 (x4)	4	Pieces	1,500	6,000
27	Miscellaneous hardware, O-rings, sealants	1	Lot	3,070	3,070
	TOTAL MATERIALS COST				**₦286,500**

2.4 Design and Construction of the Engine Test Bed

2.4.1 Structural frame and engine mounting

The structural frame was designed to support the engine, dynamometer, transmission shaft and associated equipment while maintaining adequate rigidity and shaft alignment during operation. The main RHS members were cut to the required dimensions, positioned on a flat fabrication surface and checked for squareness before welding. The main members were joined by welding, while additional cross-members and braces provided structural support. A 10 mm thick steel plate was installed as the principal mounting surface for the engine and dynamometer assemblies.

Four rubber isolation mounts were used to secure the engine to the frame. The mounts provided mechanical support and helped reduce the transmission of engine vibration to the structure. The dynamometer was mounted on a separate supporting plinth, with its input shaft aligned with the engine output shaft. The assembled frame measured approximately 2,100 mm in length and 900 mm in width.



2.4.2 Hydraulic dynamometer

A hydraulic water-brake dynamometer was fabricated to provide a controllable resisting torque against the engine output. The rotor was manufactured from mild steel plate and fitted with twelve curved vanes on each face. The rotor had a nominal diameter of 280 mm and was mounted on a 35 mm diameter EN 8 carbon-steel shaft. The housing was produced from grey cast iron and assembled around the rotor to form the working chamber.

Water was introduced into the dynamometer through an inlet connection, while a separate outlet permitted the discharge of heated water. The inlet and outlet valves were used to regulate the quantity of water within the working chamber and consequently the resistance imposed on the rotating assembly. The absorbed mechanical energy was dissipated predominantly as heat in the working water, making continuous water circulation necessary during testing. The dynamometer housing was supported on trunnion bearings, allowing the housing to react to the torque transmitted through the rotor. A 500 mm moment arm was attached to the housing, and the reaction force was measured using a strain-gauge load cell. The absorbed torque was determined from the measured reaction force and the effective length of the moment arm.

2.4.3 Power transmission and safety provisions

Mechanical power was transmitted from the engine output shaft to the dynamometer through a vehicle propeller shaft fitted with universal joints. Adapter plates were used to connect the shaft to the engine and dynamometer. The shaft arrangement permitted limited angular misalignment between the connected rotating components.

A sheet-metal guard was fabricated around the exposed rotating shaft and coupling assembly. The installation also incorporated an emergency-stop control and an exhaust pipe to discharge combustion products away from the immediate test position. The engine was inspected before testing, and its lubricating oil, coolant and spark plugs were renewed. The cooling system, fuel connections, electrical instrumentation and shaft connections were checked before the engine was started.

2.5 Test Engine

A Toyota 7A-FE petrol engine removed from a 2001 Toyota Corolla AE111 was used to evaluate the test bed. The engine was a naturally aspirated, four-cylinder, four-stroke, in-line engine with electronic fuel injection and a nominal displacement of 1,762 cm^3. The bore and stroke were 79.0 mm and 90.0 mm, respectively, and the compression ratio was 9.5:1. The thesis recorded a service mileage of approximately 96,000 km. Before installation, the engine was inspected and the cylinder compression pressures were measured. The reported readings ranged from 1,150 to 1,220 kPa across the four cylinders. Spark plugs, engine oil, coolant and the air-filter element were renewed before testing. The engine was subsequently secured to the test-bed mounting points and coupled to the dynamometer.

The engine was selected because it provided a representative four-cylinder petrol engine for evaluating the test bed within its intended application range. Published factory specifications recorded in the thesis were used as a reference for subsequent comparison with the experimentally determined performance characteristics. Such comparisons were interpreted with consideration of the engine's service history and the operating conditions during testing.

2.6 Instrumentation and Calibration

Calibration was performed before the performance tests to establish the relationship between instrument readings and the corresponding physical quantities. The procedures were based on the calibration methods documented in the thesis, with reference to the measurement-accuracy requirements of ISO 1585:2020.

2.6.1 Torque-measurement system

The torque-measurement system consisted of a strain-gauge load cell connected to a moment arm with an effective length of 0.500 m. The load cell was calibrated by applying known masses at the same effective point at which the dynamometer reaction force was measured. The corresponding force values were calculated from the applied masses, and the digital display readings were recorded.

2.6.2 Engine-speed measurement

Engine speed was measured using an optical tachometer directed towards a reflective strip on the rotating coupling flange. The tachometer was checked against a reference stroboscope at selected speeds of 1,500, 3,000 and 5,000 rpm. The observed readings were compared with the corresponding reference values to assess agreement over the operating range.

The thesis reports a maximum deviation of approximately 0.5% during these checks. The optical tachometer was subsequently used to measure engine speed during both full-load and part-load testing.

2.6.3 Fuel-consumption measurement

Fuel consumption was measured using a graduated 5 L burette connected to the engine fuel supply through a three-way valve. During a measurement, the valve was switched from the normal fuel supply to the burette, and the volume of fuel consumed over a measured interval was recorded. Fuel density was determined for the fuel batch used, with the thesis reporting a value of 0.726 kg/L at an ambient temperature of 29°C.

The fuel mass flow rate was calculated from the measured fuel volume, fuel density and elapsed time, as expressed in Equation (1):

The equation for the fuel mass flow rate is:

$$\dot{m}_f = \frac{\rho_f V_f}{\Delta t} \quad (1)$$

Where:

$\dot{m}_f = fuel\ mass\ flow\ rate\ (kg/s)$

$\rho_f = fuel\ density\ (kg/m^3)$

$V_f = volume\ of\ fuel\ consumed\ (m^3)$

$\Delta_t = measurement\ interval\ (s)$

The volume and time units were converted to a consistent SI basis before calculating the mass flow rate. The original burette readings and stopwatch records were retained as the primary data for subsequent calculation of fuel consumption and engine efficiency.

2.6.4 Temperature measurement

Type K thermocouples connected to digital indicators were used to monitor coolant outlet temperature and exhaust-gas temperature. The coolant temperature was monitored to establish whether the engine had reached a stable thermal condition before measurements were recorded. Exhaust-gas temperature was monitored to provide an indication of the variation in exhaust thermal conditions with engine speed and load.

2.7 Experimental Procedure

2.7.1 Preliminary checks and engine warm-up

Before each test series, the engine mounting bolts, shaft coupling, rotating-shaft guard, fuel lines, water connections, lubrication system and instrumentation were inspected. The engine was started and allowed to warm up under a light dynamometer load. The thesis specifies a warm-up period of approximately 15 minutes at 2,000 rpm, until the coolant outlet temperature stabilised within the reported range of 82-88℃. The water-brake dynamometer was supplied continuously with cooling water during operation. Water flow and loading were adjusted through the inlet and outlet valves to establish the required operating conditions. Readings were taken only after the engine speed and thermal conditions had stabilised.

2.7.2 Full-load performance test

The full-load test was conducted with the engine throttle fully open. The dynamometer load was adjusted to maintain the selected engine speed while the engine operated at full throttle. Ten nominal speed points were specified: 1,000, 1,500, 2,000, 2,500, 3,000, 3,500, 4,000, 4,500, 5,000 and 5,500 rpm.

At each test point, the water-brake loading was adjusted until the desired speed was reached and maintained. Following the stabilisation period, the engine speed, load-cell force, fuel consumption, coolant temperature and exhaust-gas temperature were recorded. The thesis reports that three sets of readings were taken at each speed point over a 90-second period and averaged for subsequent analysis.

The nominal measurement procedure was informed by ISO 1585:2020, which requires torque, speed and temperature to remain substantially stable before readings are taken and specifies accuracy requirements for the measurement systems. Nevertheless, because the thesis does not establish that every ISO requirement was met, the experimental procedure is reported as a laboratory full-load test rather than a fully standardised engine-certification test.

2.7.3 Part-load performance test

Part-load testing was conducted at a nominally constant engine speed of 3,000 rpm. The throttle opening was varied to four nominal positions: 25%, 50%, 75% and 100%. At each throttle position, the dynamometer load was adjusted to maintain the target engine speed, and measurements were taken after a stabilisation period of approximately 60 seconds.

The recorded variables included engine speed, torque, fuel consumption, coolant temperature and exhaust-gas temperature where applicable. The resulting measurements were used to examine the variation in brake power, fuel consumption and fuel-efficiency parameters with throttle opening. This procedure provided a comparison of engine performance under different loading conditions at a common nominal speed.

2.8 Data Reduction and Performance Calculations

The raw measurements were processed to determine brake power, brake-specific fuel consumption and brake thermal efficiency. The calculations were based on the measured torque, engine speed, fuel mass flow rate and the calorific value of the test fuel.

2.8.1 Brake power

Brake power was calculated from the measured torque and engine speed using Equation (2):

The equation for brake power is:

$$BP = \frac{2\pi NT}{60{,}000} \quad (2)$$

Where:

$BP = brake\ power\ (kW)$

$N = engine\ speed\ (revolutions\ per\ minute, rpm)$

$T = engine\ torque\ (N.m)$

2.8.2 Brake-specific fuel consumption

Brake-specific fuel consumption represents the mass of fuel consumed per unit of brake energy output. It was calculated using Equation (3): The equation for brake-specific fuel consumption (BSFC) is:

$$BSFC = \frac{\dot{m}_f \times 3600}{BP} \quad (3)$$

Where:

$BSFC = brake - specific\ fuel\ consumption\ (g/kWh)$

$3600 = conversion\ factor\ from\ seconds\ to\ hours$

Lower BSFC values indicate that less fuel mass is required to produce a unit of brake energy under the corresponding operating condition.

2.8.3 Brake thermal efficiency

Brake thermal efficiency was calculated as the ratio of useful brake energy output to the chemical energy supplied by the fuel. Using BSFC in g/kWh, Equation (4) was applied: The equation for brake thermal efficiency is:

$$\eta_{bth} = \frac{3.6 \times 10^6}{BSFC \times CV} \times 100 \quad (4)$$

Where:

$\eta_{bth} = brake\ thermal\ efficiency\ (\%)$

$CV = calorific\ value\ of\ the\ fuel\ (kJ/kg)$

$3.6 \times 10^6 = conversion\ factor\ accounting\ for\ the\ energy\ units\ used\ in\ the\ calculation.$

2.8.4 Comparative performance assessment

The calculated full-load torque and brake-power values were compared with the published factory specifications reported for the Toyota 7A-FE engine. The comparison considered the maximum measured torque, maximum measured brake power and the corresponding engine speeds.

The analysis also examined the variation in BSFC and brake thermal efficiency across the full-load speed range and across the four throttle positions at 3,000 rpm. The purpose of this comparison was to describe the engine's measured operating characteristics and assess the utility of the fabricated test bed for steady-state performance evaluation.

The measured and calculated parameters were organised in tables and plotted against engine speed or throttle position, as appropriate. The performance curves were interpreted in terms of the relationships among engine speed, torque, brake power and fuel consumption. No inferential statistical tests were specified because the investigation primarily involved the design and experimental evaluation of a single test engine.

2.9 Safety and Experimental Limitations

Safety precautions included guarding the rotating propeller shaft and coupling, checking the security of the engine and dynamometer mounts, inspecting fuel and cooling-water connections, maintaining exhaust extraction and providing emergency-stop controls. Continuous cooling-water circulation was necessary to remove heat generated during dynamometer operation.

The study was limited to one used Toyota 7A-FE petrol engine, steady-state full-load testing over the specified speed range and part-load testing at a nominal speed of 3,000 rpm. The instrumentation did not include direct measurement of intake-air mass flow, in-cylinder pressure or exhaust emissions. Consequently, the study focused on the performance parameters derivable from the recorded torque, speed and fuel-consumption measurements.

The experimental assessment also did not constitute a complete durability, fatigue or maximum-capacity test of the dynamometer. The design rating of 90 kW should therefore be interpreted separately from the maximum brake power measured during the reported engine tests.

3. RESULTS AND DISCUSSION

3.1 Instrumentation Calibration and Measurement Reliability

The calibration results indicated that the instrumentation system was suitable for conducting preliminary steady-state engine performance tests. The strain-gauge load cell was calibrated using

known masses applied at the torque measurement point. The calibration exhibited a linear relationship, with a reported slope of 0.998 and a coefficient of determination (R^2) of 0.9999. These results indicate close agreement between the applied reference loads and the instrument response over the calibration range.

The optical tachometer was compared with a reference stroboscope at 1,500, 3,000 and 5,000 rpm, with a reported deviation within ±0.5%. The fuel burette was checked gravimetrically, while the thermocouples were compared with reference temperature instruments. The reported uncertainties were ±0.5% for the burette, ±1.5°C for coolant temperature and ±5°C for exhaust temperature.

Table 3 Summary of instrumentation calibration results

Instrument	Calibration method	Reported result
Strain-gauge load cells	Dead-weight calibration	$Slope = 0.998; (R^2 = 0.9999)$
Optical tachometer	Comparison with reference stroboscope	Deviation with $\pm 0.5\%$
Fuel burette	Gravimetric volume check	Error within $\pm 0.5\%$
Coolant thermocouple	Comparison with reference thermometer	$\pm 1.5\%$
Exhaust thermocouple	Comparison with reference thermocouple	5℃

The calibration results are consistent with the instrumentation approach adopted by Romandoni et al. (2021), who developed a water-brake dynamometer using a load cell for torque measurement and a rotational sensor for engine-speed measurement. Similarly, Hamada et al. (2022) employed a hydraulic dynamometer equipped with a load-cell measurement arrangement in their investigation of the performance and emissions of a multi-cylinder spark-ignition engine. These studies demonstrate the suitability of combining force and rotational-speed measurements for engine performance assessment.

However, calibration alone does not establish the complete accuracy of an engine test bed. The uncertainty associated with the torque arm length, alignment, coupling losses, speed fluctuations and repeatability of the measured quantities should also be considered. The present calibration results therefore provide evidence of instrument-level consistency but should not be interpreted as proof of full compliance with an engine-testing standard.

3.2 Full-Load Engine Performance

The full-load test was conducted with the throttle fully open over an engine-speed range of 1,000-5,500 rpm. Torque was calculated from the measured load-cell force and the 0.5 m moment arm, while brake power was calculated from torque and rotational speed.

Table 4 Measured torque, calculated brake power and exhaust temperature at full load

Engine speed (rpm)	Measured torque (N·m)	Calculated brake power (kW)	Exhaust temperature (℃)
1,000	80.5	8.4	215
1,500	99.5	15.6	270
2,000	114.0	23.9	328
2,500	126.5	33.1	389
3,000	135.5	42.6	445
3,500	132.5	48.6	480
4,000	127.5	53.4	520
4,500	118.5	55.9	558
5,000	107.0	56.0	592
5,500	90.0	51.8	618

3.2.1 Torque–speed relationship

The measured torque increased from 80.5 N·m at 1,000 rpm to a maximum of 135.5 N·m at 3,000 rpm. Above this speed, torque decreased progressively to 90.0 N·m at 5,500 rpm. This behaviour demonstrates that the engine developed its highest measured torque within the mid-speed operating range rather than at its maximum test speed.

The increase in torque at lower and intermediate speeds may be associated with improvements in cylinder filling and combustion effectiveness as engine speed increases from idle-region operation. Beyond the peak-torque region, the time available for cylinder filling decreases and mechanical and gas-exchange losses become increasingly important. These effects can contribute to the observed reduction in torque at higher speeds.

The measured maximum torque of 135.5 N·m occurred at 3,000 rpm, compared with the factory figure of 151 N·m at 2,800 rpm reported in the thesis. The measured value is approximately 10.3% below the stated factory value. The difference in peak-torque speed is 200 rpm.

This trend is broadly consistent with published engine-dynamometer studies. Kraisoda (2020), in a study of a prototype disc-brake dynamometer, reported that torque increased to a maximum at approximately 2,500 rpm before declining as engine speed increased. Hamada et al. (2022) also reported a speed-dependent torque and performance response during full-throttle and partial-throttle testing of a multi-cylinder spark-ignition engine. Although the engines and test arrangements differ, the reported trends support the general observation that torque does not increase indefinitely with rotational speed.

The difference between the present measurements and the factory specification should nevertheless be interpreted cautiously. The tested engine was a used unit, and the thesis does not establish that its condition, fuel, atmospheric conditions and correction procedures were identical to those used for the original manufacturer rating. Consequently, the measured difference cannot be attributed exclusively to engine wear.

3.2.2 Brake power-speed relationship

Brake power increased from 8.4 kW at 1,000 rpm to approximately 56.0 kW at 5,000 rpm. It then decreased to 51.8 kW at 5,500 rpm. The maximum measured brake power therefore occurred at 5,000 rpm, close to the stated factory-rated power speed of 5,200 rpm. The increase in power despite declining torque between 3,000 and 5,000 rpm is consistent with the relationship between brake power, torque and rotational speed:

$$P_b = \frac{2\pi NT}{60{,}000} \qquad (5)$$

As rotational speed increases, power can continue to rise even when torque begins to decline, provided that the increase in speed compensates for the reduction in torque.

The measured maximum power of approximately 56.0 kW is about 13.8% below the factory rating of 65 kW reported in the thesis. This difference is similar in magnitude to the torque difference, although the two quantities peak at different engine speeds. The results indicate that the test bed was able to produce a coherent torque–speed and power–speed profile over the tested range.

Romandoni et al. (2021) reported the design and development of a water-brake dynamometer intended for testing a 118 cm³ engine, with torque measured using a load cell and engine speed measured using a rotational sensor. Kraisoda (2020) also demonstrated the use of a prototype brake dynamometer to determine torque and brake power from engine-speed measurements. The present work extends this general approach to a substantially larger, 1.8 L, four-cylinder petrol engine and a test-bed design intended for a higher power range.

Nevertheless, the highest experimentally observed power of approximately 56.0 kW should be distinguished from the test bed's design rating of 90 kW. The experiment demonstrates operation

at the reported test points; it does not independently demonstrate that the dynamometer can continuously absorb 90 kW under all operating conditions.

3.3 Exhaust Temperature Characteristics

The exhaust temperature increased progressively from 215℃ at 1,000 rpm to 618℃ at 5,500 rpm. The temperature rose at each successive test speed, even after torque began to decline beyond 3,000 rpm. This indicates that the exhaust-gas thermal condition was strongly influenced by engine speed and the rate at which fuel energy was released during operation. The increasing exhaust temperature at higher speeds may reflect greater fuel consumption per unit time and a larger rate of energy transfer through the exhaust stream. However, exhaust temperature alone cannot determine the fraction of fuel energy lost through the exhaust. Such an assessment would require additional measurements, including exhaust mass flow, air-fuel ratio and fuel-energy input.

The observed temperature trend is consistent with the importance of exhaust temperature as an engine-performance parameter in published experimental studies. Hamada et al. (2022) examined performance and emissions under different throttle conditions using a hydraulic dynamometer, demonstrating the value of assessing engine operating variables together rather than interpreting torque or power in isolation. The present study adds exhaust-temperature monitoring to the locally fabricated test bed, making it potentially useful for practical teaching and further combustion-related investigations. The maximum recorded exhaust temperature of 618℃ at 5,500 rpm should be interpreted in relation to the sensor location, engine operating duration and measurement uncertainty. As the thesis reports a thermocouple uncertainty of ±5℃, the values are best treated as measured estimates rather than exact exhaust-gas temperatures.

3.4 Part-Load Performance at 3,000 rpm

Part-load testing was carried out at a nominal constant engine speed of 3,000 rpm, with throttle openings of approximately 25%, 50%, 75% and 100%. The torque and brake-power values reported in the thesis are presented in Table 5.

Table 5 Reported part-load performance at 3,000 rpm

Throttle opening (%)	Torque (N·m)	Brake power (kW)
25	38.5	12.1
50	74.5	23.4
75	108.5	34.1
100	135.5	42.6

The results show a progressive increase in torque and brake power with increasing throttle opening. Torque increased from 38.5 N·m at 25% throttle to 135.5 N·m at full throttle, while brake power increased from 12.1 to 42.6 kW. This represents an approximately 252% increase in torque and a 252% increase in brake power between the lowest and highest throttle settings.

The observed trend is physically expected for a throttled spark-ignition engine. Increasing throttle opening generally allows a greater mass of air–fuel mixture to enter the cylinders, enabling higher cylinder pressure and greater useful work per engine cycle. Conversely, restricting the throttle reduces the inducted charge and increases the relative influence of pumping losses.

The findings agree qualitatively with Hamada et al. (2022), who reported better brake mean effective pressure, brake-specific fuel consumption and brake thermal efficiency under wide-open-throttle conditions than under partial-throttle operation in their tested multi-cylinder petrol engine. Their results also demonstrated that throttle position is an important variable in engine-performance testing.

The comparison is qualitative rather than a direct numerical validation because the engine specifications, test conditions and instrumentation differ between studies. In addition, the throttle percentages in the present work were approximate mechanical positions rather than verified percentages of inducted airflow or engine load. Therefore, the results should be interpreted as a comparison of four throttle settings at nominally constant speed, not as a linear relationship between percentage throttle and engine output.

3.5 Comparison with Published Studies and Manufacturer Data

The performance characteristics obtained in this study can be compared with published dynamometer-development studies and the factory performance values reported for the Toyota 7A-FE engine.

Table 6 Comparison with selected published work

Study	Test engine or system	Relevant reported finding	Relationship to the present study
Romandoni et al. (2021)	Water-brake dynamometer designed for a 118 cm³ engine	Load-cell torque measurement and rotational-speed sensing were incorporated into a compact dynamometer design	Supports the instrumentation principle used in the present water-brake test bed
Kraisoda (2020)	Prototype disc-brake dynamometer tested with a small petrol engine	Maximum torque was reported near 2,500 rpm and maximum power near 3,000 rpm	Demonstrates the use of measured torque and speed to establish engine performance curves
Hamada et al. (2022)	Multi-cylinder spark-ignition engine coupled to a hydraulic dynamometer	Engine performance varied with speed and throttle opening; wide-open-throttle operation generally provided better performance indicators than	Supports the observed effects of engine speed and throttle opening on torque and brake power

		partial-throttle operation	
Present study	Toyota 7A-FE, 1.8 L, four-cylinder petrol engine	Maximum measured torque of 135.5 N·m at 3,000 rpm and maximum calculated brake power of approximately 56.0 kW at 5,000 rpm	Demonstrates steady-state testing of a larger automotive engine using the fabricated test bed

The principal contribution of the present work is the design, fabrication and experimental use of a locally constructed water-brake engine test bed for a 1.8 L automotive engine. In contrast to the smaller-engine applications described by Romandoni et al. (2021) and Kraisoda (2020), the present test arrangement was designed for four-cylinder petrol engines in the 1.2–2.0 L range. The use of a fabricated structural frame, hydraulic absorption unit, strain-gauge load cell and optical tachometer provides a practical platform for engine-performance demonstrations and controlled steady-state tests.

The comparison with Hamada et al. (2022) is particularly relevant to the part-load findings because both studies considered a multi-cylinder spark-ignition engine and changes in throttle opening. However, the present study should not claim equivalent measurement accuracy or standards compliance solely because similar instrumentation was used. Such a claim would require documented uncertainty analysis, repeatability statistics and confirmation that the test procedure met the relevant requirements.

3.6 Economic Evaluation of the Fabricated Test Bed

The bill of materials in the thesis reports a direct material cost of ₦286,500. This cost covers the structural steel, dynamometer components, shaft and bearings, instrumentation, fuel-measurement equipment, cooling components, protective guard and associated fabrication materials. Labour, workshop facilities and overhead costs were excluded.

The reported material cost suggests that local fabrication may provide a practical route to acquiring engine-testing equipment in institutions where the capital cost of commercial test facilities is a constraint. The result is relevant to the educational application of the equipment, particularly for practical instruction in engine performance, torque measurement, brake-power calculation and the influence of engine operating conditions.

However, the economic claim should be limited to the documented direct material expenditure. A full cost comparison with commercial equipment would require current quotations for comparable systems with equivalent power capacity, measurement accuracy, control capability, safety provisions, installation requirements and after-sales support. Without such quotations and a consistent scope of comparison, the reported cost cannot independently establish a precise percentage saving against imported equipment.

3.7 Data-Quality Considerations and Implications for Interpretation

Although the torque and brake-power trends are internally consistent with the measured force and rotational speed, the fuel-related results in the thesis require reconciliation before publication.

The thesis reports fuel volumes measured over 60 seconds, corresponding fuel masses, fuel mass-flow rates, BSFC values and brake thermal efficiencies. However, these quantities do not consistently agree dimensionally. For example, at 3,000 rpm, the recorded fuel mass of 11.8 g over 60 seconds corresponds to a mass-flow rate of approximately 0.197 g/s. Combining this value with a brake power of 42.6 kW gives a BSFC of approximately 16.6 g/kWh using the stated formula. This value is not physically credible for a conventional petrol engine and indicates that the recorded fuel measurement interval, mass units or calculation basis may be incorrect.

The reported thermal-efficiency values are consequently not suitable for interpretation until the original fuel readings and calculation procedure have been verified. The same caution applies to any comparison of the present BSFC values with published engine studies. A valid comparison requires the fuel mass-flow rate, brake power and lower heating value to be expressed on consistent units and a common calculation basis.

There is also a discrepancy between the thesis abstract, which reports a maximum torque of 141 N·m, and the full-load measurement table, which reports 135.5 N·m at 3,000 rpm. The abstract and results should be reconciled using the original experimental records. In addition, the brake-power values should be recalculated directly from the final validated torque and speed measurements, and the brake mean effective pressure values should be independently checked before inclusion in the manuscript.

These issues do not negate the observed torque–speed and power–speed trends, but they limit the conclusions that can currently be drawn from fuel economy and thermal efficiency. The final manuscript should clearly distinguish verified measurements from derived values that remain subject to correction.

3.8 Overall Discussion

The results demonstrate that the fabricated test bed was used to obtain steady-state torque, brake-power and exhaust-temperature measurements from a Toyota 7A-FE petrol engine over a speed range of 1,000–5,500 rpm. The torque curve reached a maximum of 135.5 N·m at 3,000 rpm, while the calculated brake power peaked at approximately 56.0 kW at 5,000 rpm. At a nominal speed of 3,000 rpm, increasing throttle opening produced a progressive increase in torque and brake power.

These trends agree qualitatively with published dynamometer studies showing that engine performance varies with rotational speed and throttle position. The instrumentation and hydraulic loading approach also follows established practice in water-brake dynamometer development. The locally fabricated design therefore provides a potentially useful platform for practical engine testing and engineering education.

Nevertheless, the evidence supports a conclusion about demonstrated operation at the reported test points, rather than proof of the full 90 kW design capacity. Further work should include

repeatability and uncertainty analysis, independent verification of the fuel-consumption measurements, confirmation of the load-cell capacity and a documented comparison with a reference dynamometer. These steps would strengthen the reliability of the performance data and the case for adopting the equipment for research and teaching.

4. CONCLUSION AND LIMITATIONS OF THE STUDY

4.1 Conclusion

This study successfully demonstrated the design, construction and experimental evaluation of a locally fabricated automotive engine test bed incorporating a hydraulic water-brake dynamometer. The test bed was developed for testing four-cylinder petrol engines within the 1.2–2.0 L displacement range, with a design absorption rating of 90 kW and a maximum design torque of 220 N·m. The system incorporated a mild-steel supporting frame, a water-brake power-absorption unit, a strain-gauge load cell for torque measurement, an optical tachometer for engine-speed measurement, and instrumentation for monitoring fuel consumption and engine temperatures.

Performance evaluation was conducted using a Toyota 7A-FE 1.8 L, four-cylinder petrol engine over a speed range of 1,000–5,500 rpm. The recorded measurements showed that torque increased with engine speed up to a maximum reported value of 135.5 N·m at 3,000 rpm, before declining at higher speeds. Brake power increased progressively and reached approximately 56.0 kW at 5,000 rpm. During part-load testing at 3,000 rpm, both torque and brake power increased with increasing throttle opening. These trends demonstrate the usefulness of the fabricated system for investigating the relationship between engine speed, throttle position, torque and brake power under steady-state operating conditions.

The reported calibration results also indicated a strong linear response from the load-cell system and close agreement between the optical tachometer and its reference instrument. The test bed therefore provides a practical platform for engineering education, engine-performance demonstrations and further experimental investigations. The reported direct material cost of ₦286,500 suggests the potential affordability of local fabrication, although a comprehensive economic comparison would require verified quotations for commercially available systems with equivalent specifications. Overall, the study establishes the feasibility of constructing and operating a locally developed engine test bed for automotive performance testing. However, the experimental results demonstrate performance only over the conditions tested; the full design absorption capacity of 90 kW has not been experimentally verified. Furthermore, the fuel-consumption, brake-specific fuel-consumption and brake thermal-efficiency calculations require validation against the original experimental records before these parameters can support definitive conclusions.

The study was limited by the use of a single, previously used Toyota 7A-FE engine, meaning that the findings may not be directly generalisable to other engine designs, displacement classes or operating conditions. The evaluation focused primarily on steady-state operation within the tested

speed range and did not establish the test bed's performance under transient loading, long-duration operation or the full 90 kW design rating. Although the principal measuring instruments were calibrated, a comprehensive uncertainty analysis incorporating load-cell response, moment-arm dimensions, shaft alignment, speed variation and measurement repeatability was not fully established. In addition, the study did not include direct measurements of intake-air mass flow, air–fuel ratio, in-cylinder pressure, exhaust emissions, vibration or noise. The reported fuel-consumption and derived efficiency values also contain inconsistencies that require resolution using the original measurements and calculation records. Finally, the reported material cost excludes labour, workshop facilities and overheads, limiting the conclusions that can be drawn about the total construction cost and comparative economic advantage. Future studies should address these limitations through independent validation against a reference dynamometer, repeated tests under controlled conditions, a formal measurement-uncertainty assessment, verified fuel-flow calculations, and evaluation across multiple engines and a broader range of operating conditions.

References

Hamada, K. I., Rahim, M. F., Rahman, M. M., & Bakar, R. A. (2022). Throttling effect on the performance and emissions of a multi-cylinder gasoline fuelled spark ignition engine. International Journal of Automotive and Mechanical Engineering, 19(4), 10084–10093. https://doi.org/10.15282/ijame.19.4.2022.05.0779

International Organization for Standardization. (2020). Road vehicles—Engine test code—Net power (ISO Standard No. 1585:2020). https://www.iso.org/standard/70078.html

Kraisoda, P. (2020). Prototype of disc brake dynamometer. Research Square. https://doi.org/10.21203/rs.3.rs-30894/v1

Romandoni, N., Aminudin, A., Faizin, K. N., Puspitasari, I., Salim, A. T. A., & Aziz, A. (2021). Design of water brake dynamometer. Journal of Physics: Conference Series, 1845(1), Article 012048. https://doi.org/10.1088/1742-6596/1845/1/012048

Winarko, A. (2013). Rancang bangun engine water brake dynamometer sebagai media pembelajaran praktek pengujian performa mesin. Jurnal Teknik Mesin, 1(2). https://ejournal.unesa.ac.id/index.php/jtm-unesa/article/view/928